Estimation of spectral amplification coefficients of seismic motion in Greece and comparison with the corresponding coefficients of the 2024 draft, "Eurocode 8".

Chatzianagnostou E.[1,2], Theodoulidis N.[2], Grendas I.[2], Hatzidimitriou P.[1], Triantafyllidis P.[1]

[1]Aristotle University of Thessaloniki (AUTH)

[2]Institute of Engineering Seismology and Earthquake Engineering (I.T.S.A.K.)

Abstract

This study proposes an integrated approach to evaluate Spectral Amplification Factors (SAFs) at sites, down to seismological ($H_{3km/s}$) and engineering ($H_{800m/s}$) bedrock. Six reference stations of ITSAK accelerometer network have been selected, positioned on 'rock' formations as per surface geology. Research's core lies in the joint inversion of ambient noise horizontal to vertical spectra ratio (mHVSR) recordings and dispersion curves data under the Diffuse Field concept, attempting to develop 1D-Vsz profiles in those six reference stations, reaching down to the seismological bedrock of the site ($Vs_{3km/s}$). The transfer function derived from these profiles were employed in the deconvolution of the Fourier Amplitude Spectra (FAS) of earthquake surface recordings across Greece, down to seismological and engineering ($Vs_{800m/s}$) bedrock. The deconvolved FAS are utilized in a parametric Generalized Inversion Technique (GIT), to estimate the horizontal and vertical SAFs for $H_{800m/s}$ and compare them for $H_{3km/s,}$ for 152 station sites. Additionally, the HSAFs derived from the GIT, then classified according to soil type based on the 2024 draft of Eurocode 8 (EC8) and compared to the respective amplification factor proposed by EC8. Finally, the log- average of Vertical Amplification Correction Function (VACF), by using the estimated HSAFs from GIT and the earthquake HVSR data, was calculated, aiming at the blindly estimation of HSAFs at a site, exclusively based on eHVSR. Results of this study are promising to estimate HSAF based on measured eHVSR at a site. In addition, spectral amplification factors after their respective categorization, show satisfactory agreement with those of EC8. However, further research is needed to quantify and improve uncertainties observed in the above comparisons.

Methodology and Data used

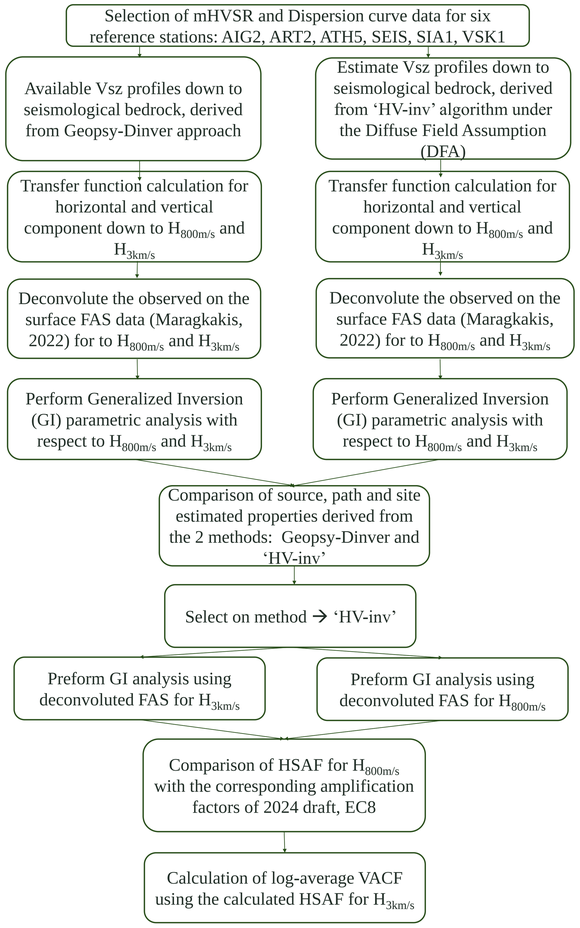

Figure 1: Schematic flowchart depicting the methods used and the steps followed in this study.

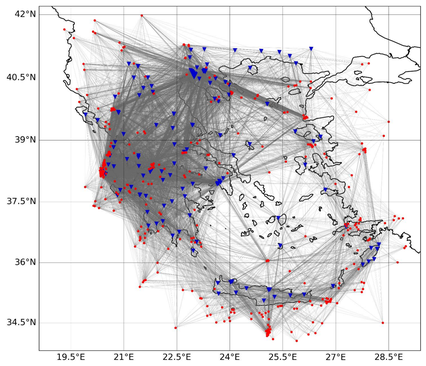

Figure 2: Ray-paths derived for seismic events for subcentral distances that constitute the observed FAS data file before the correction of sites

In this study, we explore the inversion of the Horizontal to Vertical (H/V) spectral ratio of ambient noise under the Diffuse Field Assumption, DFA (Sanchez-Sesma et al., 2008, Petron et al., 2009), using 'HV-inv' algorithm (Garcia – Jerez et al. 2016) which allow separate computation of the contributions of P, SH, SV and Rayleigh , Love surface waves.

The Generalized Inversion Technique (GIT) for earthquake recording, first proposed by Andrews, 1986, Iwata and Irikura, 1988 and Castro et al., 1990. This method allows for a comprehensive investigation of the source, path and site properties within the frequency domain, when there are numerous earthquake data available. The uniform earthquake recordings catalogue (observed FAS) were compiled by Maragkakis, 2022, using HAN's accelerometer data, focused on records where the 12km ≤ Rhyp ≤ 300km, 4 ≤ Mw ≤ 6, H(focal) ≤ 40km and PGA ≤ 200 cm/s^2.

Generalized Inversion technique (GIT)

Source parameters

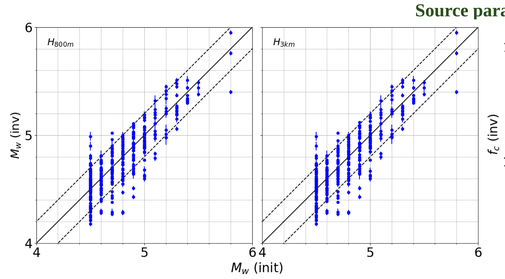

Figure 3: Observed Moment Magnitude (Mw (init)) versus inversion calculated Moment magnitude (Mw (inv)), down to $H_{800m/s}$ (left) and $H_{3km/s}$ (right). The dashed lines depict the misfit of the estimated Mw (inv) values.

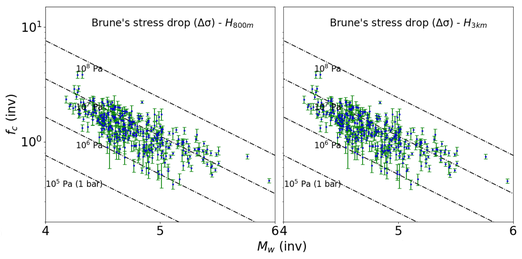

Figure 4: Comparison of the inversion calculated corner frequencies, fc and the computed Mw, alongside with the Brune's stress drop lines, down to $H_{800m/s}$ (left) and $H_{3km/s}$ (right).

Fourier amplitude spectra from surface earthquake recordings were corrected through deconvolution, down to seismological and engineering bedrock with Vs of 3km/s and 800m/s, respectively, employing the Transfer Functions (TF) derived from Vsz profile for 6 reference stations. These deconvolved data are used in the Generalized Inversion (GI) process, from which the key factors of seismic source, path, and site properties have been calculated.

Overall, 372 shallow earthquakes were analyzed within the designated area, in and around Greece, with magnitudes ranging from 4.5 to 5.8. From GIT the Mw were re-calculated and plotted alongside with the observed Mw as well as with the corner frequency, fc.

An important frequency independent factor is the quality factor, Q_0 (for 1Hz and Rhyp ≤ 300km), related to path properties, which was evaluated for 241 distinct cells in a delimited area in and around Greece, for $H_{800m/s}$ and $H_{3km/s}$. In figure 5, on top, the coefficient of variation (CV), which is expressed as a percentage, is being illustrated. A lower CV percentage indicates greater precision in the coefficient's estimation of results. On bottom, the Q_0 values are depicted only when the corresponding CV was lower or equal than 7%. The two cases scenarios, $H_{800m/s}$ (right) and $H_{3km/s}$ (left), are juxtaposed, revealing a strong agreement across the entire frequency spectrum.

Site effects

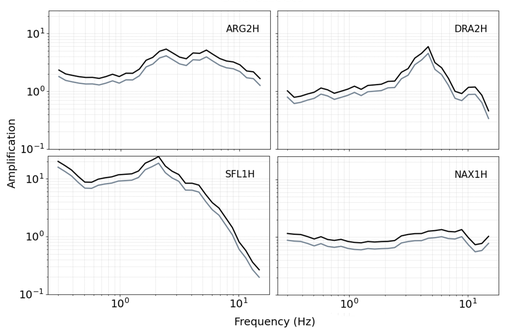

Path properties

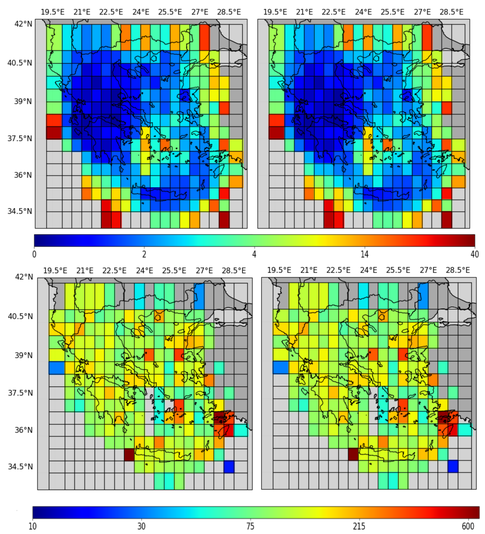

Figure 5: Maps corresponding to the variation of coefficient variation, CV (top) of quality factor (Q_0 for 1Hz) and the smoothed Q_0 for CV<7% (bottom) for $H_{800m/s}$ (right) and $H_{3km/s}$ (left).

Finally, the HSAFs and VSAFs were computed for frequency range 0.3 Hz – 15 Hz. There is a noticeable deamplification almost consistent, along the frequence windows, for SAFs down to engineering bedrock.

Figure 6: The HSAFs for 4 stations across Greece. The black curves represent the factors down to $H_{3km/s}$, while the grey curves represent the factors down to $H_{800m/s}$.

Comparison with EC8 and VACF calculation

HSAFs derived from GI analysis, for $H_{3km/s}$, has been used, along with the eHVSR data on the surface, to evaluate the logarithmic average of the Vertical Amplification Correction Function (VACF), ± a standard deviation, for 152 sites (figure 7). The equation from which the VACF is calculated is:

$$VACF = \frac{HSAF}{eHVSR}$$

Figure 7: Variation of the log-average empirical VACF for all 152 stations (black lines)) ± 1 std, in comparison with the curves calculated for the Japanese area (blue lines) ± 1 std, by Ito et al., 2020

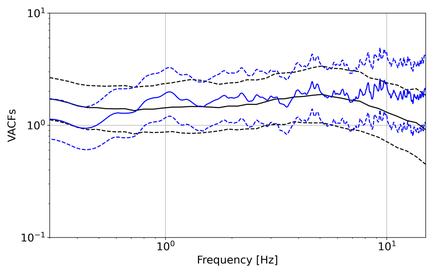

Additionally, HSAFs for each station, were utilised in the categorisation per soil type according to EC8. The final categorisation showed a noticeable concentration of HSAFs (around 70%) in category B (very dense sand, gravel, or very stiff clay) (figure 8).

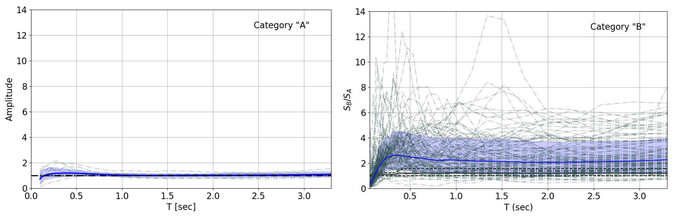

Figure 8: Left: The elastic design spectra for ground type A (black line, ± std dashed black lines). The dashed grey curves are the SAFs grouped in category A, while the blue line is the log-average of those SAFs with std (shadowed blue). Right: Ratios of elastic design spectra with respect to ground type A according to EC8 (black lines, ± std dashed black lines) for category B. The dashed grey curves are the SAFs grouped in category B. The blue line is the log-average of SAFs with std (shadowed blue).

Conclusions

A crucial aspect of the study was to compare the Generalized Inversion (GI) results for $H_{800m/s}$ and $H_{3km/s}$. The analysis showed almost negligible differences in the factors related to seismic source and path. However, in terms of site factors (both horizontal and vertical), there was an observed increase of about 30% across the entire frequency range when the inversion extended down to the seismological bedrock ($H_{3km/s}$).

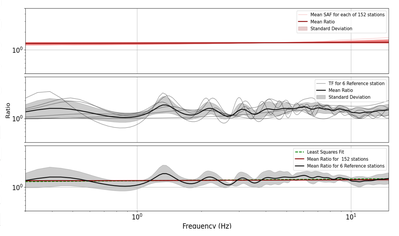

Figure 5: Top: TF ratio ($TF_{3km/s}/TF_{800m/s}$) (from GIT) with log-average and std. Middle: TF ratio (from 1D-Vsz profiles) with log-average and std. Bottom: Combined log-averages, std, and least squares fit.

Furthermore, the pronounced clustering of amplification factors in a single category (B) according to EC8, prompts questions regarding the flexibility and the broader applicability of how a category is defined.

Finally, the log-average VACF calculated for 152 stations across Greece exhibit amplification within the frequency range of 2.0 Hz to 8 Hz, similar to the values calculated by Ito et al. 2021, while for frequencies lower than 0.5 Hz, unexpected values greater than 1.0 were observed, indicating a potential issue requiring further investigation. Conversely, at frequencies higher than 8Hz a steep reduction in VACF values is observed, that could be linked to the Soil-Structure-Interaction (SSI) of buildings housing the accelerometer stations. This phenomenon also warrants further investigation.

References

- D.J. Andrews. Objective determination of source parameters and similarity of earthquakes of different size. Earthquake Source Mechanics, 37:259 – 267, 1986
- R.R. Castro, J.G. Anderson, and S.K. Singh. Site response, attenuation and source spectra of s waves along the Guerrero, Mexico, subduction zone. Bulletin of the Seismological Society of America, 80(6A):1481 1503, 1990.
- Garcıa-Jerez, J. Pina-Flores, F.J. Sanchez-Sesma, F. Luzon, and M. Petron. A computer code for forward calculation and inversion of the H/V spectral ratio under the diffuse field assumption. Computers and Geosciences, 97:67–78, 2016
- E. Ito, K. Nakano, F. Nagashima and H. Kawase. A Method to Directly Estimate *S* -Wave Site Amplification Factor from Horizontal-to-Vertical Spectral Ratio of Earthquakes (eHVSRs). *Bulletin of the Seismological Society of America*, 110(6), pp. 2892–2911. 2020.
- T. Iwata and K. Irikura. Source parameters of the 1983 Japan sea earthquake sequence. Journal of Physics of Earth, 36(4):155–184, 1988.
- Maragkakis I.. Site Amplification Factors in station of the National Network of Accelometers in Greece. Master Thesis. 2022.
- M. Petron, F.J. Sanchez-Sesma, A. Rodriquez-Castellanos, M. Campillo, and R.L. Weaver. Two perspectives on equipartition in diffuse elastic fields in three dimensions. The Journal of the Acoustical Society of America, 126:1125–1130, 2009.
- F.J. Sanchez-Sesma, J.A. Perez-Ruiz, F. Luzon, M. Campillo, and A. Rodrıguez- Castellanos. Diffuse fields in dynamic elasticity. Wave Motion, 45(5):641–654, 2008.

Acknowledgements

This study is based on a part of a Master dissertation program in Applied Geophysics and Seismology at Aristotle University of Greece "Estimation of spectral amplification coefficients of seismic motion in Greece and comparison with the corresponding coefficients of the 2024 draft, "Eurocode 8". This study has partially funded by the "ARGONET+" project.

Chatzianagnostou E. echatzian@gmail.com
Theodoulidis N. ntheo@itsak.gr
Grendas I. grendasioannis@gmail.com
Hatzisimitriou P. chdimitr@geo.auth.gr
Triantafyllidis P. trian@geo.auth.gr